PROCEEDINGS of the
23rd International Congress on Acoustics
9 to 13 September 2019 in Aachen, Germany

Clustering in an array of nonlinear and active oscillators as a model of spontaneous otoacoustic emissions

Liv Moretto Sørensen[(1)], Peter Leer Bysted[(2)], Bastian Epp[(3)]

[(1)]Niels Bohr Institute, University of Copenhagen, bvf365@alumni.ku.dk
[(2)]Department of Health Technology, Technical University of Denmark, s144045@student.dtu.dk
[(3)]Department of Health Technology, Technical University of Denmark, bepp@dtu.dk

Abstract

Spontanoeus otoacoustic emissions (SOAEs) are sound signals emitted by the inner ear of many species in the absence of an external stimulus. The precise mechanism underlying the generation of SOAEs is still unknown. This paper investigates the phenomenon of frequency clustering in a system of coupled, nonlinear oscillators as a possible mechanism underlying the generation of SOAEs. A generic system consisting of 100 Van der Pol oscillators was implemented with dissipative and reactive coupling elements of varying strength. Frequency clusters were investigated in terms of size, frequency and phase coherence as a function of coupling strength and scaling of the nonlinearity. One configuration of the modelled system was synchronised by an external driving force. Phase relations between oscillators were analysed and compared both before and after synchronisation. Frequency clusters appeared for some configurations of the coupled system. Dissipative coupling resulted in clusters of equal frequency spacing and similar size, while reactive coupling resulted in fewer clusters and much more complex dynamics of the resulting system. Even though the phenomenon of frequency clustering is well described in the literature, less is known about both the phase relation and coherence within and across clusters. These two factors play an important role in the generation of the observed SOAEs and might help to identify the criticial parameters of the underlying mechanism in inner ear mechanics.

Keywords: Cochlea, SOAE, nonlinear dynamics, otoacoustic emission, oscillators

1 INTRODUCTION

The human ear's ability to detect extremely small differences in sound levels and to discriminate frequencies with high precision has yet to be explained fully. It was argued in [6] that it would not be possible to achieve the healthy ear's sensitivity with passive mechanisms. In this connection the presence of an active mechanical feedback mechanism in the ear was postulated, often referred to as the "active process" [13, 5]. This was supported by the discovery of the spontaneous otoacoustic emissions (SOAEs) [7, 15]. SOAEs are sound signals that can be measured in the absence external stimuli, pointing towards self-sustained activity in the inner ear, possibly linked to outer hair cell motility [1]. An interesting characteristic of these emissions are the narrow distributions of energy in the spectra of the emitted signal. SOAEs are vulnerable to a damage of outer hair cells and tend to disappear even for mild hearing impairment [10]. Although the lizard basilar papilla shows a simpler structure than the human cochlea, the SOAEs share some interesting characteristics [2]. Hence lizard inner ear models might provide important insights for mammalian SOAE generation [13, 5]. It was reported [8] that SOAEs in bobtail lizards contain roughly 10 evenly spaced peaks in the power spectrum. This number of peaks is much lower than the number of hair cells in the bobtail lizard. Under the assumption that outer hair cells play a key role, it is therefore believed that numerous cells must be synchronised within the basilar papilla to produce sound with the characteristics of SOAEs. A model that has been of main interest in the investigation of the active process in the inner ear is a system of nonlinear, active, coupled limit cycle oscillators [11]. This was first suggested by [6] and modeled in different varieties [4, 3, 13, 5, 14]. These models can account for many key aspects of the phenomena observed in SOAEs, including effects of entrainment. Entrainment is the phenomenon that causes oscillators with different natural frequencies to group in clusters with neighbouring

oscillators, all oscillating at the same frequency [9]. This phenomenon can either be triggered by intrinsic oscillations within the system or by an external driving force. Even though both systems of coupled oscillators and SOAEs are well investigated, the methods to quantify the observations differ. In order to transfer insights from one field to the other, the implications, differences, and similarities of the various analysis methods need to be linked in order to draw conclusions about the underlying mechanisms. The only way to analyse SOAEs in the ear canal is by means of Fourier analysis while it is common to describe nonlinear dymamics with the help of, e.g., phase diagrams. Because only one state variable is available for SOAEs (the pressure in the ear canal) the assumption of a periodic oscillation is commonly made, even though nonlinear and active oscillators often shown non-harmonic dynamics. In this paper, a model- and analysis framework inspired by previous models of coupled, nonlinear, active oscillators is described. A system of coupled Van der Pol oscillators [12, 9] is created to investigate the changes in behaviour both globally and locally while the parameters that define the dynamics and the coupling between oscillators are varied. Specifically, the effects of dissipative and reactive coupling between nearest neighbours are investigated with focus on the formation of clusters. These clusters are analysed with respect to size, stability and phase coherence. Synchronisation effects are quantified with respect to cluster size and cluster frequency.

2 METHODS

2.1 Model

The modeled system consisted of $N = 100$ Van der Pol oscillators, each described by the equation of motion:

$$\ddot{x} = -\omega^2 x + \mu(1-x^2)\dot{x} \tag{1}$$

where x is the displacement from equilibrium, $\dot{x}$ and $\ddot{x}$ are the velocity and acceleration, respectively. The factor μ scales the nonlinearity of the system. In the case $\mu = 0$, the eigenfrequency $\omega = \sqrt{K/M}$ of the oscillator is defined by the spring constant K and the mass M (for this study, all masses were set to $M = 1$). To account for tonotopy, a linear gradient in the eigenfrequency was introduced by

$$K_\mathrm{n} = \left(\omega_\mathrm{min} + \frac{(\mathrm{n}-1)\omega_\mathrm{max}}{N-1}\right)^2 \cdot \varepsilon_\mathrm{n} \qquad \mathrm{n} \in \{1...N\} \qquad \varepsilon_\mathrm{n} = \mathcal{N}(1,\nu) \tag{2}$$

The value of K_n was varied stochastically for each oscillator by a random variable drawn from a normal distribution $\mathcal{N}$ with mean one and standard deviation ν to aid generation of clusters [9]. Because the phase plane trajectory of a Van der Pol oscillator varies both with μ and ω, a scaling of the time differential was introduced by a scaling of μ to keep the ratio ω/μ constant and to result in identical phase trajectories of all N oscillators. This yields the equation of motion for oscillator n

$$\ddot{x}_\mathrm{n} = -x_\mathrm{n} + \frac{\mu(1-x^2)}{\omega_\mathrm{n}}\dot{x}_\mathrm{n} \tag{3}$$

The force between two coupled neighbouring oscillators is given by

$$\begin{aligned} F_\mathrm{n} = {} & d_{\mathrm{n}+1}(\dot{x}_{\mathrm{n}+1} - \dot{x}_\mathrm{n}) + k_{\mathrm{n}+1}(x_{\mathrm{n}+1} - x_\mathrm{n}) \\ & + d_\mathrm{n}(\dot{x}_{\mathrm{n}-1} - \dot{x}_\mathrm{n}) + k_\mathrm{n}(x_{\mathrm{n}-1} - x_\mathrm{n}) \end{aligned} \tag{4}$$

where the dissipative and reactive coupling are described by d and k, respectively. Positions x_0 and x_{N+1} were held constant to zero. For the systems analysed in this paper, the boundary conditions were fixed, which means that oscillators $\mathrm{n} = 1$ and $\mathrm{n} = N$ are coupled to the fixed boundary points. Extending (3) with (4) and adding an external driving force, F_ext, yields a second order differential equation. This can be rewritten as a set of first

order differential equations for numerical treatment:

$$\begin{aligned} \frac{dx_{\mathrm{n}}}{dt} &= \dot{x}_{\mathrm{n}} \\ \frac{d\dot{x}_{\mathrm{n}}}{dt} &= -x_{\mathrm{n}} + \frac{\mu(1-x^2)}{K_{\mathrm{n}}}\dot{x}_{\mathrm{n}} + F_{\mathrm{n}} + F_{\mathrm{ext}} \end{aligned} \tag{5}$$

2.2 Analysis

2.2.1 Steady state criteria

The dynamics of the system was simulated for time intervals of length T_{int} and stopped as soon as a steady state of the system was reached. This state was defined by a "nearly constant" energy over time and the requirement that the minimum energy in the system must exceed a value of $10^{-2} \cdot N$. The energy of each oscillator was approximated by:

$$E_{\mathrm{n}}(m) = \sum_{t=mT_{\mathrm{int}}}^{(m+1)T_{\mathrm{int}}} x_{\mathrm{n}}(t)^2 \ , \ m = 0, 1, 2... \tag{6}$$

If $E_{\mathrm{n}}(m+1)$ did not differ from $E_{\mathrm{n}}(m)$ by more than ten percent for all n, the system was defined to be in steady state.

2.2.2 Frequency and cluster analysis

Three methods were used to analyze the frequency of each oscillator: 1) "Fourier mean method" ($\Omega_{\mathrm{f,mean}}$), computed as the weighted mean of all frequencies Ω_i in the Fourier domain, 2) "Fourier peak method" ($\Omega_{\mathrm{f,peak}}$), computed by localising the frequency with the highest normalized peak m' in the Fourier domain, and 3) the "Zero crossing mean method" ($\Omega_{\mathrm{zc,mean}}$) where the frequency was determined from the inverse of the mean distance between zero crossings Δt_{zc} in the time domain:

$$\Omega_{\mathrm{f,mean}} = \sum_i m_i' \Omega_i \quad ; \qquad \Omega_{\mathrm{f,peak}} = \Omega(\texttt{find}(m' = 1)) \quad ; \qquad \Omega_{\mathrm{zc,mean}} = \frac{1}{P} = \left(2\frac{\sum \Delta t_{\mathrm{zc}}}{n_{\mathrm{zc}}}\right)^{-1} \tag{7}$$

Clusters of minimum four oscillators were analyzed with the system in steady state. In order to qualify as a cluster, the frequency differences between oscillators within one cluster must have been smaller than half the frequency difference between to neighboured oscillators assuming a linear gradient between the natural frequencies of the two oscillators with lowest and highest index n in the cluster:

$$\mathrm{step}_{\mathrm{cluster}} < \frac{(\Omega_{\mathrm{high}} - \Omega_{\mathrm{low}})}{2N}$$

where frequencies Ω_{high} and Ω_{low} can be found using any of the frequency analysis methods mentioned above. The phase coherence of the oscillators was computed using the estimated oscillation period combined with the amplitude and velocity of each oscillator. The normalized [displacement, velocity]-vectors after each oscillation period were added in the phase plane and divided by the number of periods the oscillator has gone through.

2.3 Numerical evaluation

The coupled equations of motion were solved using MATLAB's built in `ODE45` solver. For all simulations, values in (2) were set to

$$N = 100 \ , \ \omega_{\mathrm{min}} = 2\pi \ , \ \omega_{\mathrm{max}} = 5 \cdot 2\pi \tag{8}$$

The sampling frequency was set to $f_s = 1000$Hz and the maximum step size used by `ODE45` to 0.01s. The simulation was run in intervals of length $T_{\mathrm{int}} = 20$s until the system met the steady state criteria or until the maximum simulation time of 1000s was reached. All oscillators had initial displacement and velocity equal to

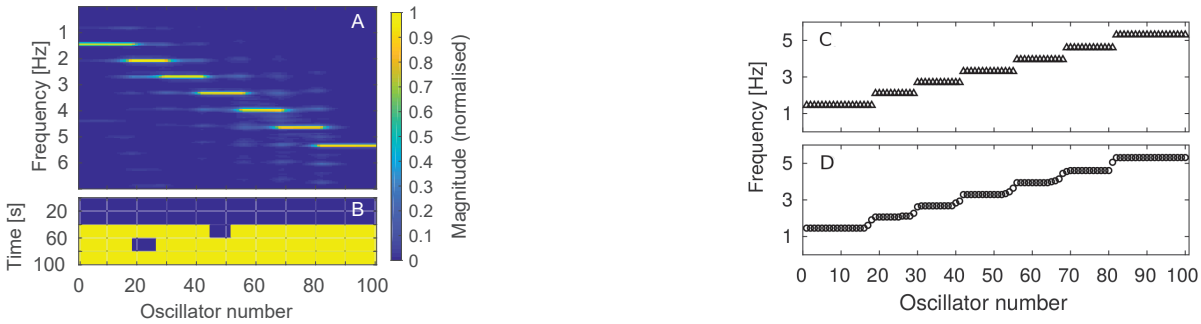

Figure 1. System $\underline{P_d}$. A) Spectral representation of the system dynamics. A 20 s steady state time interval was windowed using a Hann window prior to Fourier transformation. The spectrum for each oscillator was normalised to its maximum value to improve the graphical representation. B) State of each oscillator as function of time (in intervals of length $T_{int} = 20$s). Steady state criteria are met for values of 1 and are not met for values of 0. C) Clusters found when analysed using $\Omega_{\text{f,peak}}$. The system exhibited a regular cluster structure for the seven equally spaced clusters. The cluster size was biggest at the ends of the row of oscillators. D) Clusters for analysis with $\Omega_{\text{zc,mean}}$. Here some oscillators were located between clusters, showing intermediate cluster structure.

0 and were excited by a short rectangular pulse at time $t = 0$s with width $w = 0.05$s and unity height. The systems were analysed for parameter combinations $\underline{P} = \{d,k,\mu,\nu\}$. To get a more explicit understanding of the impact of dissipative and reactive coupling, systems were coupled by either dissipative or reactive coupling elements of varying strength. The following parameters were used for the simulations:

$$d \in \{0,1,2,5,10,20,50,100\}, \quad k \in \{0,1,2,5,10,20,50,100\}, \quad \mu \in \{0.5,1,1.5\ \ldots\ 4,4.5,5\}, \quad \nu \in \{0,0.1\} \quad (9)$$

In the absence of stochastic variations of K_n (i.e., $\nu = 0$) the system was simulated once, otherwise 25 times. The system with dissipative coupling $\underline{P_d} = \{100,0,1,0\}$ and the system with reactive coupling $\underline{P_k} = \{0,20,1,0\}$ will be described in more detail because they showed the most comprehensive clustering behaviour.

To analyse synchronisation effects by an external driving force, a force $F_{\text{ext}} = F_{\text{sin}}$ was applied to all oscillators:

$$F_{\text{sin}}(t) = \alpha \sin(2\pi f t)$$

with α the amplitude and f the frequency of the sinusoidal force. The cluster size and -frequencies were analysed as a function of both α and f:

$$f_d \in \{0,0.25,0.5\ \ldots\ 6.5,6.75,7\}, \quad f_k \in \{0,0.25,0.5\ \ldots\ 9.5,9.75,10\}, \quad \alpha \in \{0,1,10,50,100,150\}$$

with f_d and f_k denoting the frequencies of the forces driving $\underline{P_d}$ and $\underline{P_k}$, respectively.

3 RESULTS

3.1 Dissipative coupling

Figure 1A shows the spectral analysis of system $\underline{P_d}$ in steady state (reached after 80s of simulation, see Figure 1B). Clusters appeared at frequencies between 1 Hz to 5.5 Hz with equal spacing and size. This representation shows harmonics of each oscillator at frequencies of neighbouring clusters. The clusters overlap at the cluster edges, indicating two dominant frequencies for these oscillators. When extracting clusters using $\Omega_{\text{f,peak}}$ (Figure 1C), all oscillators were assigned to a cluster. Analysis of the same data with $\Omega_{\text{zc,mean}}$ (Figure 1D), resulted in a collection of oscillators that was not discrete but more smooth with some oscillators in between clusters, consistent with [9].

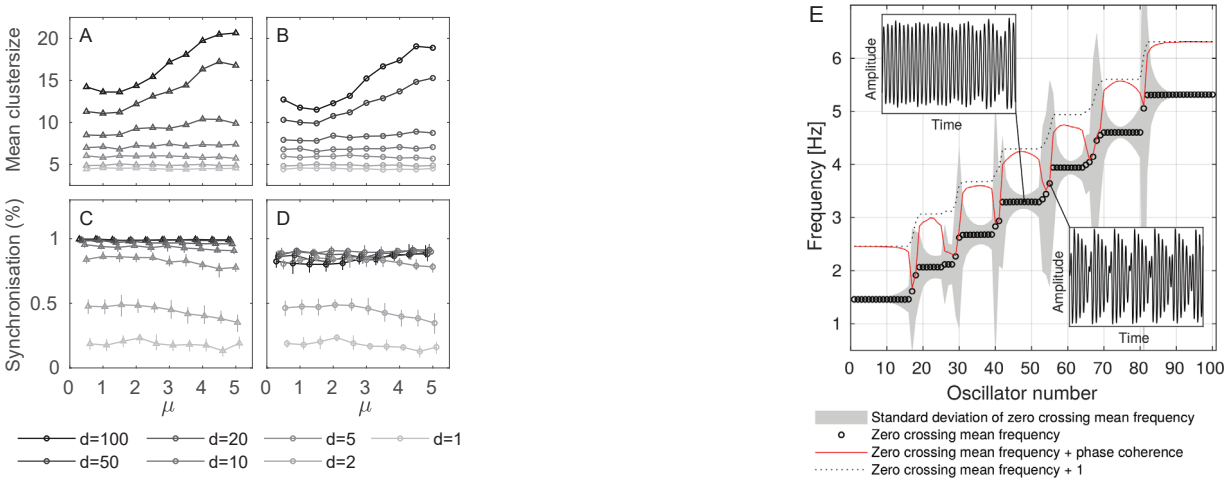

Figure 2. A-D) Mean cluster size, the number of oscillators being part of a cluster (expressed as synchronisation) for systems with varied combinations of coupling strength d and nonlinearity μ and two methods of frequency analysis (Fourier mean method, A,C; zeros crossing mean method, B,D). E) Cluster analysis using $\Omega_{\text{zc,mean}}$ with estimates of the standard deviation of the estimated frequency (grey), the estimated phase coherence (red) and the temporal dynamics of two selected oscillators (insets) of system $\underline{P_d}$ in steady state.

The number and size of the found clusters depended on the combination of coupling strength (d_n), the value of the of nonlinearity parameter μ and the method used to analyze the dominant oscillation period of each oscillator. Figure 2 shows the size and stability of the oscillation period (expressed as synchronization) of identified clusters for different combinations of d_n and μ for $\Omega_{\text{f,peak}}$ (A,C) and $\Omega_{\text{zc,mean}}$ (B,D). Larger clusters were found for stronger coupling and for higher degrees of nonlinearity. The mean cluster size and the synchronization were slightly larger when using $\Omega_{\text{f,peak}}$ compared to $\Omega_{\text{zc,mean}}$. While the maximum synchronization for $\Omega_{\text{f,peak}}$ was close to 1, the maximum value for $\Omega_{\text{zc,mean}}$ was around 0.8.

The dynamics of the oscillators within a cluster or at the corners of a cluster are shown in Figure 2E for the zero crossings mean method. The phase coherence in the middle of clusters is much higher than at the borders, where the uncertainty on the frequency analysis is correspondingly higher. The temporal dynamics showed a clear beating of one oscillator located between two clusters, consistent with two dominant frequencies as indicated in Figure 1.

3.2 Synchronization with harmonic driving force

For the phase analysis the central cluster of system $\underline{P_d}$ was used. This cluster consisted of 11 oscillators with a mean frequency of 3.3 Hz. The phase analysis of each oscillator in each cluster is shown in the absence (upper panel) and presence (lower panel) of an external driving force in Figure 3. The phase is shown for each time period $p = 1/3.3$s during the time interval T_{int} for each oscillator. In both cases, the first and last oscillators showed a much wider spread of phases compared to the oscillator in the middle of the cluster. The spread of phase is consistent with the estimate of the phase coherence (red lines). Furthermore, the mean of the phase distribution changed along the oscillators in the analysed cluster, from a mean phase of around $5/4\pi$ for oscillator 42 and a mean phase of around $1/3\pi$ for oscillator 52.

In the presence of an external driving force with frequency 3.25 Hz and amplitude $\alpha = 10$, the cluster grows in size and the phase distributions of all oscillators become more narrow. Especially in the middle of the cluster, the phases collapse into a very narrow region around the mean, indicating a very stable oscillation period. Neighboured oscillators show though a slight shift in mean phase, similar to the result in the absence of the

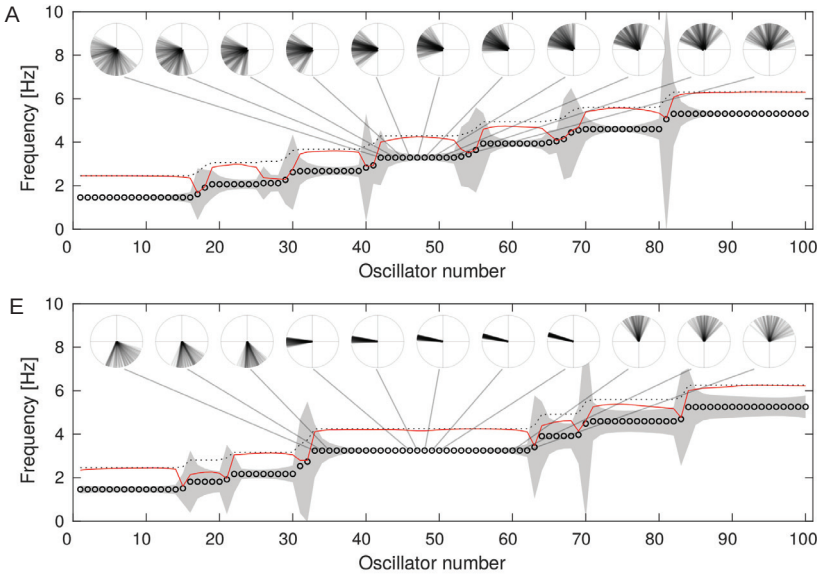

Figure 3. A) Phase analysis of the central cluster in the system $\underline{P_d}$ in steady state. The cluster consisted of oscillators $n = 42$ to $n = 52$. The mean frequency of the cluster was 3.3 Hz. The phase of each oscillator was investigated by marking points in phase space for each time period $p = 1/3.3$ s. Same legend as in 2. B) Phase analysis of central cluster in the system $\underline{P_d}$ when in steady state while being synchronised by external force with frequency $f = 3.25$ Hz and amplitude $\alpha = 10$. The cluster consisted of oscillators $n = 33$ to $n = 62$.

external driving force.

3.3 Reactive coupling

Figure 4 shows the spectral analysis of a system using reactive coupling (A,B) and an analysis of cluster size- and synchronization analogue to Figure 2. Two big clusters with frequencies around $f_l = 3.5$Hz and $f_h = 9$Hz are apparent in Figure 4A. The cluster frequency around 9 Hz was higher than the maximum eigenfrequency in the uncoupled system, indicating a contribution of the coupling elements to the dominant frequency of the oscillators. Inbetween the clusters, the oscillators showed a complex distribution of energy and no consistent clustering behaviour. Consistent with the results using dissipative coupling, clusters tended to be larger for higher amount of coupling and higher degree of nonlinearity, but the behaviour was much more complex (Figure 4C-F). The high variability in the synchrony of the single oscillators (panels D,F) are consistent with the complex distribution of energy found in the spectral analysis of the system (panel A). These results indicate a more complex dynamics and impact on the resulting frequencies when using reactive instead of dissipative coupling.

4 DISCUSSION

For systems with dissipative coupling, similar cluster patterns compared to both [13, 5, 4] appeared in the systems. Although no frequency analysis method has been defined by [13], their results show a high similarity to the results in the current study using $\Omega_{\text{f,peak}}$. The result that stronger coupling results in larger clusters (Figures 2,4) can be explained by assuming that the interaction across oscillators happens exclusively through this parameter. With increasing magnitude, the eigenfrequency of each oscillator and the local mechanical parameters play a decreasing role. Close by oscillators will start to synchronize and, as a compound effect, increase the

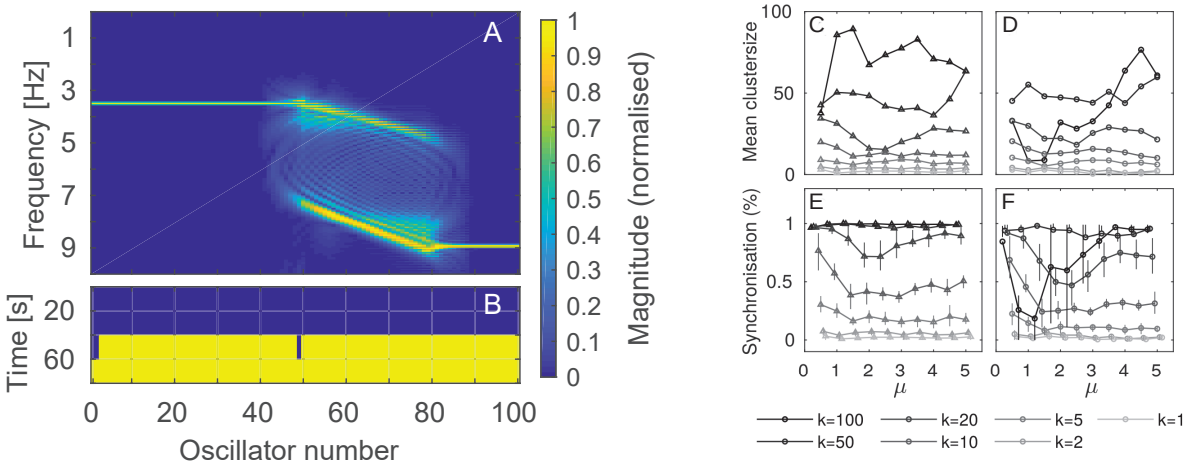

Figure 4. A-B) Same as Figure 1, but for system $\underline{P_k}$ with reactive coupling. C-F) Same as in 2, but for variations of reactive coupling constant k.

effect on neighboring oscillators. This will be the case until the balance between across-oscillator and local oscillator effects will balance and move towards the next oscillator cluster. Given that clustering is an effect of active, nonlinear oscillators, it is also intuitive that increasing the amount of nonlinearity increases the effect of clustering, leading to larger clusters.

Regarding the reactive coupling, similarities to the data presented by [4] can be observed in the spectral representation in terms of some clearly defined clusters and some more blurry areas between the clusters. Consistent with this, [5] found that the number of clusters decreases for bigger values of the reactive coupling coefficient, which might be connected to the increasing mean cluster size documented in this paper. One argument why reactive coupling shows a more complex behaviour compared to dissipative coupling is that the coupling spring constants will affect the local eigenfrequency and hence the local tuning and by that the frequency gradient across oscillators.

The often neglected information of oscillator clusters is the phase relation across oscillators within one cluster. With the results in Figure 3 it becomes clear that even though oscillators might be entrained to a specific frequency, the local properties of the oscillators will have an effect on the phase relation within a cluster. For phenomena that represent the compound result of a whole cluster like SOAEs measured in the ear canal, this phase shift will have important consequences on the measured magnitude. The measured magnitude can hence not be used to estimate the size of the cluster because the addition of phase-delayed components will reduce the resulting compound amplitude, in the extreme case to zero for components in anti phase. Phase distributions are, in general, more narrow for oscillators located centrally in a cluster that for oscillators remote from the cluster center. This might be connected to frequency difference between the cluster frequency and the eigenfrequency of the local oscillator. An external driving force heavily reduces the width of the phase distributions, making them very narrow for oscillators in the center of the cluster. It is, however, interesting to note that the phase shift of oscillators within a cluster remains the same as in the absence of the external driving force.

5 CONCLUSIONS

A system of coupled Van der Pol oscillators with a frequency gradient showed clustering effects for both dissipative and reactive coupling. The number of and distance between clusters is dependent on the magnitude and type of the coupling between oscillators. Hence, the distance observed between SOAEs might provide information about the type and strength of coupling in the inner ear. The size and frequency of clusters depends,

however, on the metric used to quantify the oscillation period of each oscillator. Finally, oscillators within one cluster showed a linear phase gradient. Hence, a better understanding of the parameters defining this phase gradient and the interaction with the size and frequency distance of clusters is required to be able to link these properties to analogue characteristics observed in SOAEs.

ACKNOWLEDGEMENTS

This work was supported by the William Demant foundation through a travel grant (LMS). We would like to thank Mogens Høgh Jensen for constructive discussions about this project.

References

[1] J. Ashmore. Cochlear outer hair cell motility. *Physiological Reviews*, 88(1):173–210, 2008.

[2] C. Bergevin and A. Salerno. Dynamics of spontaneous otoacoustic emissions. *Aip Conference Proceedings*, 1703(1):090024, 2015.

[3] B. Epp, J. L. Verhey, and M. Mauermann. Modeling cochlear dynamics: Interrelation between cochlea mechanics and psychoacoustics. *Journal of the Acoustical Society of America*, 128(4):1870–1883, 2010.

[4] B. Epp, H. Wit, and P. van Dijk. Clustering of cochlear oscillations in frequency plateaus as a tool to investigate soae generation. *Aip Conference Proceedings*, 1703(1):090025, 2016.

[5] M. Gelfand, O. Piro, M. O. Magnasco, and A. J. Hudspeth. Interactions between hair cells shape spontaneous otoacoustic emissions in a model of the tokay gecko's cochlea. *Plos One*, 5(6):e11116, 2010.

[6] T. Gold. Hearing. ii. the physical basis of the action of the cochlea. *Proceedings of the Royal Society of London. Series B - Biological Sciences*, 135(881):492–498, 1948.

[7] D. Kemp. Stimulated acoustic emissions from within human auditory-system. *Journal of the Acoustical Society of America*, 64(5):1386–1391, 1978.

[8] C. Köppl and G. Manley. Spontaneous otoacoustic emissions in the bobtail lizard .1. general-characteristics. *Hearing Research*, 71(1-2):157–169, 1993.

[9] G. V. Osipov, J. Kurths, and C. Zhou. Synchronization in oscillatory networks. 2007.

[10] R. Probst, B. Lonsbuty-Martin, and G. Martin. A review of otoacoustic emissions. *Journal of the Acoustical Society of America*, 89(5):2027–2067, 1991.

[11] C. Talmadge, A. Tubis, H. Wit, and G. Long. Are spontaneous otoacoustic emissions generated by self-sustained cochlear oscillators. *Journal of the Acoustical Society of America*, 89(5):2391–2399, 1991.

[12] B. van der Pol. Lxxxviii.on relaxation-oscillations. *London, Edinburgh, and Dublin Philosophical Magazine and Journal of Science*, 2(11):978–992, 1926.

[13] A. Vilfan and T. Duke. Frequency clustering in spontaneous otoacoustic emissions from a lizard's ear. *Biophysical Journal*, 95(10):4622–4630, 2008.

[14] H. P. Wit and P. van Dijk. Are human spontaneous otoacoustic emissions generated by a chain of coupled nonlinear oscillators? *Journal of the Acoustical Society of America*, 132(2):918–926, 2012.

[15] P. Zurek. Spontaneous narrowband acoustic-signals emitted by human ears. *Journal of the Acoustical Society of America*, 69(2):514–523, 1981.